Int. J. Electrochem. Sci., 6 **(2011)** 2566 - 2580

International Journal of
ELECTROCHEMICAL
SCIENCE
www.electrochemsci.org

Configuration Designs and Parametric Optimum Criteria of an Alkaline Water Electrolyzer System for Hydrogen Production

Houcheng Zhang, Shanhe Su, Guoxing Lin, Jincan Chen[*]

Department of Physics, Xiamen University, Xiamen 361005, People's Republic of China
[*]E-mail: jcchen@xmu.edu.cn

Received: 2 May 2011 / *Accepted:* 5 June 2011 / *Published:* 1 July 2011

An alkaline water electrolyzer system for hydrogen production and its semi-empirical equations are directly used to analyze and optimize the performance of the system. The results obtained through thermodynamic-electrochemical analysis show clearly that for such an alkaline water electrolyzer system, there exist some optimal values of the electrolyte concentration under different operating temperatures and the Joule heat resulting from the irreversibilities inside the alkaline water electrolyzer is larger than the additional heat needed in the water splitting process. Consequently, some new configurations for utilizing the surplus heat in the alkaline water electrolyzer are put forward to improve the performance of the system. The general performance of these new configurations is discussed, from which the lower bound of the operating current density is determined. In order to further optimize the characteristics of these configurations, a multi-objective function including both the efficiency and hydrogen production rate is originally put forward and used to determine the upper bound of the operating current density. The optimum criteria of main parameters and the optimally working region of the alkaline water electrolyzer system are given. In addition, the effects of some important parameters on the performance of the system are analyzed in detail.

Keywords: Alkaline water electrolyzer, overpotentials, configuration design, multi-objective function, parametric optimum criterion

1. INTRODUCTION

Hydrogen energy is expected to be useful as the secondary energy in the near future, for example as a fuel for transportation, electricity generation in fuel cells, or other applications [1-8]. Unfortunately, the vast majority of hydrogen used today is produced by fossil-fuel-based processes which may result in gas emissions such as CO_x, SO_x and NO_x. On the other hand, the fossil-fuel-based hydrogen production processes are both subject to large price fluctuations and a limit in global supply [9-12]. The development of renewable, efficient and economical hydrogen production technologies to

replace fossil-fuel-based hydrogen production methods is key step towards a sustainable "hydrogen economy" [13-16].

Water electrolysis integrated with photovoltaics, nuclear power stations or wind turbines is one of the most promising methods for large-scale renewable hydrogen production [17-20]. The electrolysis of aqueous alkaline solutions has historically been one of the most popular routes for hydrogen production [21-24]. Recently, most studies related to alkaline electrolysis emphasize on the development of new advanced electrocatalyst materials [25-29] and the increase in the operating temperature of the electrolysis cell [9, 19, 30, 31]. Comparatively, the detailed systematical configuration design and parametric optimum are rare in the current literature, but they are of importance for better understanding the performance improvement and operating mechanism of an alkaline water electrolyzer and worthwhile to be further studied.

In the present paper, we evaluate and analyze the performance of an alkaline water electrolyzer system for hydrogen production, based on its semi-empirical equations, and structure some new configurations of an alkaline water electrolyzer system so that the redundant heat in the alkaline water electrolyzer may be utilized. The performance characteristics of these new configurations are discussed and optimized. Some significant results are obtained.

2. THE POWER INPUT OF AN ALKALINE WATER ELECTROLYZER SYSTEM

The schematic diagram of an alkaline water electrolyzer system for hydrogen production is shown in Fig. 1.

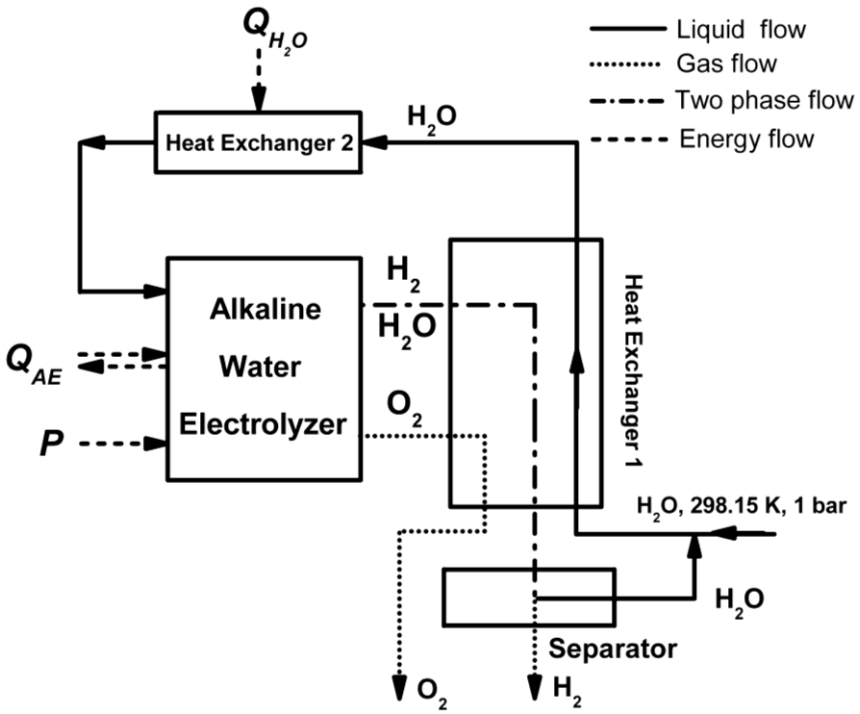

Figure 1. The schematic diagram of an alkaline water electrolyzer system.

The system mainly consists of an alkaline water electrolyzer using circulating KOH solution as electrolyte, a separator and two heat exchangers. The model established here is general and reasonable as it can be connected to any power generation system and the waste heat contained in the products can be efficiently utilized. Water, electricity and heat, if necessary, are provided to the alkaline water electrolyzer to drive the water splitting reactions. The generated H_2 and residual H_2O flow out at the cathode and the generated O_2 flows out at the anode. Since a large fraction of the heat added to the feed water is remained in the products at the outlet, it is desirable to recover the waste heat from the products through heat exchanger 1. After leaving heat exchanger 1, O_2 is cooled down to reference condition (T_0 = 298.15 K and p_0 = 101.33 kPa) and can be used as by-product. The H_2/H_2O mixture flows into the separator, H_2 is cooled down and stored as fuel; and the hot H_2O is circulated for the next H_2 production cycle. Due to the inefficiency of exchanger 1 and different thermodynamic parameters of reactant/products, the feeding water should be further heated through exchanger 2 before reaching the temperature of the alkaline water electrolyzer.

According to Fig. 1, the overall water electrolysis reaction is that H_2O plus electricity and heat turns to H_2 and O_2, i.e., H_2O+heat+electricity$\rightarrow H_2+(1/2)O_2$. The total energy required for electrolytic hydrogen production $\Delta H(T)$ is the sum of thermal energy demand $Q(T)$ and electrical energy demand $\Delta G(T)$, i.e.,

$$\Delta H(T) = Q(T) + \Delta G(T), \quad (1)$$

where $Q(T)=T\Delta S(T)$, $\Delta S(T)$ is the entropy change in the water splitting reactions, $\Delta G(T)$ is the change in the Gibbs free energy, and T is the operating temperature of the alkaline water electrolyzer. Generally, the standard thermodynamic parameters such as $\Delta H(T)$, $\Delta S(T)$ and $\Delta G(T)$ have different values at different temperatures even under a constant pressure condition. These thermodynamic parameters can be calculated from the data in Table 1 [32-35].

Table 1. Thermodynamic parameters for the reactant/products at 101.325 kPa, where (g) and (l) represent gas phase and liquid phase, respectively.

Compound	$G(T_0)$ (J mol^{-1})	$H(T_0)$ (J mol^{-1})	$S(T_0)$ (J mol^{-1})	Heat Capacity(C_p) (J mol^{-1} K^{-1})
H_2 (g)	-38,960	0	130.68	$27.28+0.00326T+50000/T^2$
O_2 (g)	-61,120	0	205.00	$29.96+0.00418T-167000/T^2$
H_2O (l)	-306,690	-285830	69.95	75.44

For an electrochemical process operating at constant pressure and temperature, the minimum input work required is equal to the change in Gibbs energy $\Delta G(T)$. According to Faraday's law, the voltage required for a reversible electrochemical process can be expressed as [23, 24, 36, 37]

$$U_{rev} = \frac{\Delta G(T)}{n_e F}, \quad (2)$$

where n_e is the number of electrons transferred per hydrogen molecule and F is Faraday's constant.

Table 2. Parameters used in the modeling.

Parameter	Value
Faraday constant, F (C mol^{-1})	96,485
Number of electrons, n_e	2
Universal gas constant, R (J mol^{-1} K^{-1})	8.314
Low heating value of H_2, LHV (KJ mol^{-1})	241.83
Partial pressure of product H_2, P_{H_2} (atm)	1
Partial pressure of product O_2, P_{O_2} (atm)	1
Partial pressure of product H_2O, P_{H_2O} (atm)	1
Constant, c_1 (A. m^{-2})	174,512
Constant, c_2 (K)	5485
Transfer coefficient, α	0.1668
Area of single-cell polar plate, A_p (m^2)	0.064
Limiting current density, j_L (A m^{-2})	2000
Thickness of the electrolyte, t_{ele} (m)	0.01
Effectiveness of the heat exchangers, ε	0.7
Inlet flow rate of water, $N_{H_2O,in}$ (mol s^{-1})	6.6×10^{-4}
Temperature of the AFC, T (K)	353
Temperature of the external heat source, T_s (K)	400
Temperature of the environment, T_0 (K)	298.15

When a water electrolyzer comes into operation, the required voltage U is always larger than the reversible voltage U_{rev} because of the irreversibilities resulting from the water splitting reactions and may be expressed as

$$U = U_{rev} + U_{act} + U_{con} + U_{ohm}, \quad (3)$$

where $U_{act} = \frac{RT}{\alpha n_e F} \ln\left(\frac{j}{j_0}\right)$ is the activation overpotential losses related to the electrochemical kinetics [32, 36, 38], $j_0 = c_1 \exp\left(\frac{-c_2}{T}\right)$ is the exchange current density, c_1 and c_2 are constants which are independent of T, α is the transfer coefficient; $U_{con} = \frac{RT}{\alpha n_e F} \ln\left(\frac{j_L}{j_L - j}\right)$ is the concentration overpotential losses caused by mass transfer [32, 38], j_L is the limiting current density; $U_{ohm} = j\frac{t_{ele}}{k}$ is

the ohmic overpotential losses caused by the resistance of electrolyte as the resistance of electrodes can be neglected compared with that of electrolyte [32, 39], t_{ele} is the thickness of the KOH electrolyte, and k is the specific conductivity of the KOH solution. Based on the experiment data, Gilliam et al. [40] developed an equation which can be used to describe the relationship between the specific conductivity κ of aqueous KOH solution and electrolyte concentration *M*, i.e.,

$$\kappa = \frac{-2.041M - 0.0028M^2 + 0.005332MT + 207.2M/T + 0.001043M^3 - 0.0000003M^2T^2}{100}, \qquad (4)$$

which was very valid for temperatures from 0 ^{0}C to 100 ^{0}C and for KOH concentrations from 0 to 12 *M* [40].

By using Eqs. (2)-(4) and the parameters listed in Table 2 [38, 41], the electrochemical characteristics of an alkaline water electrolyzer are clearly shown in Fig. 2.

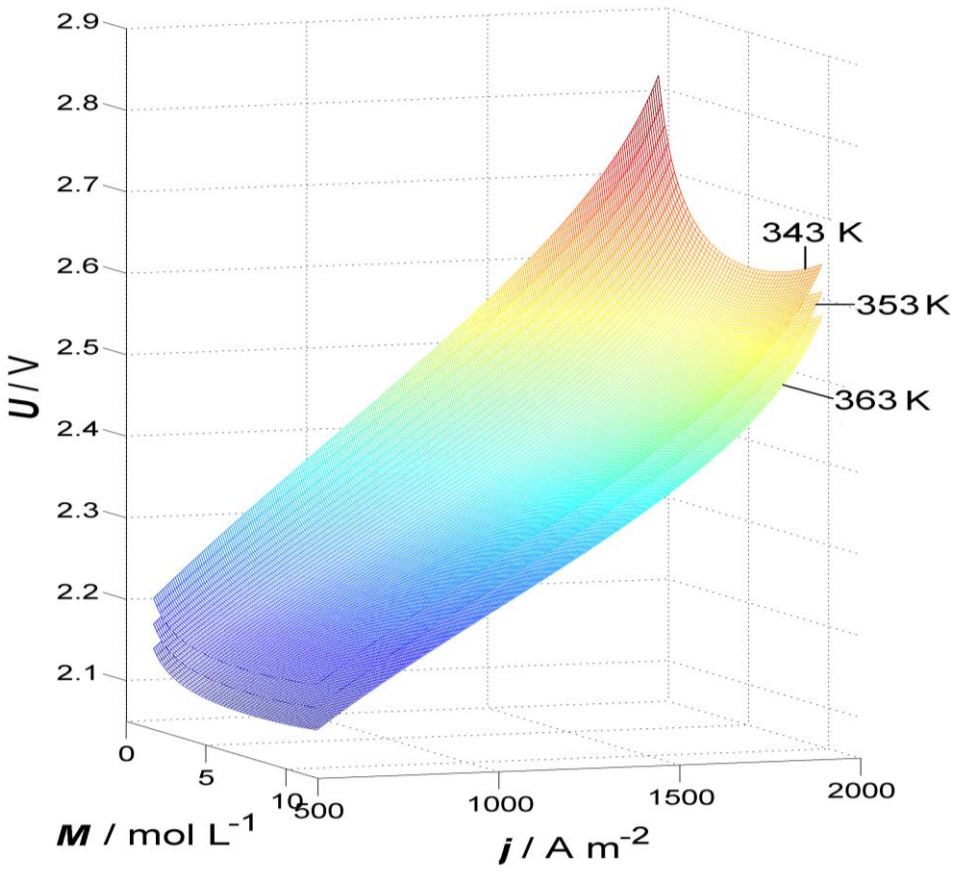

Figure 2. Three dimensional figures of the required voltage versus electrolyte concentration and current density for different operating temperatures.

It shows that the voltage required increases as the operating current density is increased, while it decreases as the operating temperature is increased. The influence of the electrolyte concentration on the required voltage is negligible when the operating current density is small and increases with the increase of the operating current density. When the alkaline water electrolyzer system is operated at high current densities, the voltage required first decrease and then increase as the electrolyte concentration is increased, and consequently, there exists a minimum input voltage, as shown in Fig. 2. By using numerical calculation, the concrete values of the optimum concentration $M_{\min}$ for some given operating temperatures are listed in Table 3. It is seen from Table 3 that $M_{\min}$ increases with the increase of the operating temperature.

Table 3. The optimal electrolyte concentrations for different operating temperatures.

T(K)	343	353	363
$M_{\min}$ (mol L^{-1})	7.383	7.543	7.671

By using Eqs.(2)-(4), the electric power required by the alkaline water electrolyzer can be expressed as

$$P = IU = \frac{I}{n_e F}[\Delta G(T) + \frac{RT}{\alpha}\ln\left(\frac{j}{j_0}\right) + \frac{RT}{\alpha}\ln\left(\frac{j_L}{j_L - j}\right) + j\frac{n_e F t_{ele}}{k}], \quad (5)$$

where $I = jA_e$ is the electric current through the alkaline water electrolyzer and A_e is the effective surface area of the alkaline water electrolyzer.

3. THE DIFFERENT CONFIGURATIONS AND EFFICIENCIES OF AN ALKALINE WATER ELECTROLYZER SYSTEM

For an alkaline water electrolyzer, the Joule heat produced per unit time may be expressed as

$$Q_J = I(U_{act} + U_{ohm} + U_{con}). \quad (6)$$

Practically, the Joule heat produced in the electrolyzer is unnecessarily released to the environment and may be directly used to supply to the water splitting reactions. Thus, the thermal energy required for the electrolyzer per unite time may be reduced from Q to

$$Q_{AE} = (Q - Q_J). \quad (7)$$

According to Fig. 1 and Refs. [33, 39, 41], the heat supplied by the external heat source for heating compensatory water can be calculated by the following equation:

$$Q_{H_2O} = \frac{N_{H_2O,in}}{\varepsilon}\int_{T_0}^{T} C_{p,H_2O}dT - \left[N_{H_2,out}\int_{T_0}^{T} C_{p,H_2}dT + N_{O_2,out}\int_{T_0}^{T} C_{p,O_2}dT + N_{H_2O,out}\int_{T_0}^{T} C_{p,H_2O}\,dT \right]$$

$$= \left[N_{H_2O,in}\left(1/\varepsilon - 1\right) + \frac{I}{2F} \right]\int_{T_0}^{T} C_{p,H_2O}dT - \frac{I}{2F}\int_{T_0}^{T}(C_{p,H_2} + \frac{C_{p,O_2}}{2})dT\,, \qquad (8)$$

where N_i are the inlet or outlet flow rates of species *i* (H_2O, H_2 or O_2), ε is the effectiveness of the heat exchanger, $C_{p,i}$ are the molar heat capacities of species *i* at one atmospheric pressure [33-35], and T_0 is the environment temperature.

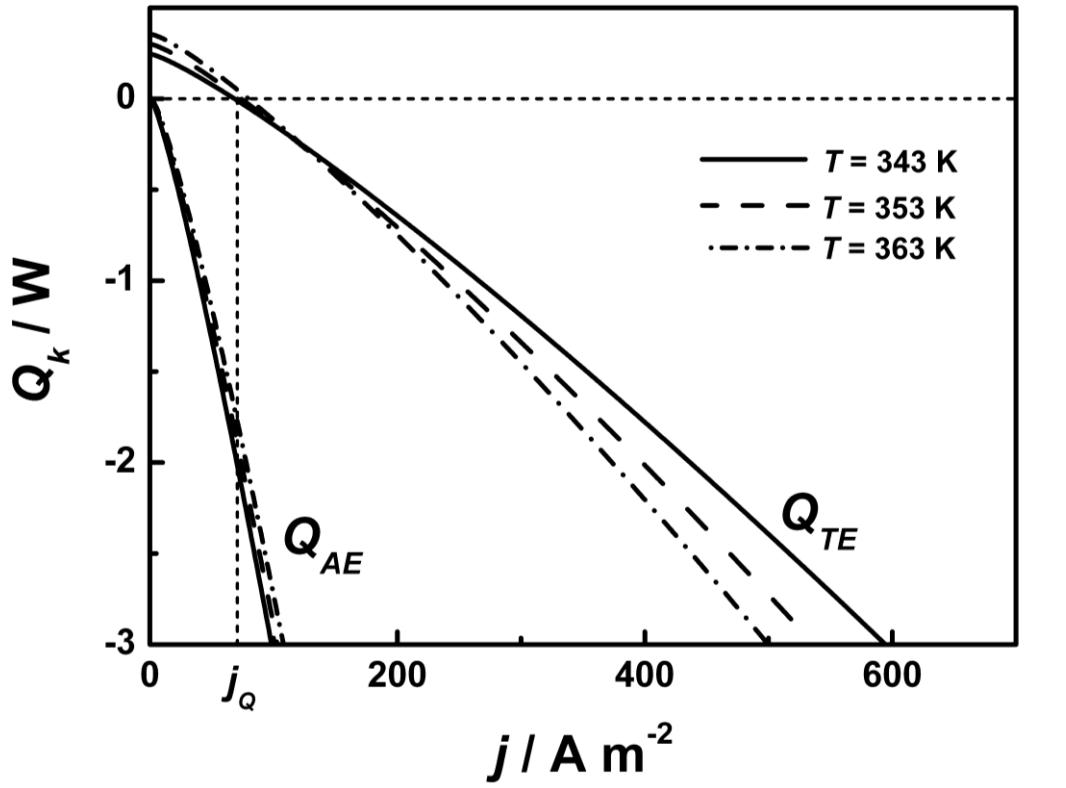

Figure 3. The curves of Q_{AE} and Q_{TE} varying with the current density for different temperatures, where $Q_{TE} = Q_{AE}(1-T_0/T) + Q_{H_2O}(1-T_0/T_s)$ and j_Q is the current density when $Q_{TE} = 0$.

It may be easily proved from Eq. (8) and the data in Tables 1 and 3 that $Q_{H_2O} > 0$. According to the above analysis, we can further obtain the curves of Q_k (*k*=*AE* and *TE*) varying with *j*, as shown in Fig. 3, where $Q_{TE} = Q_{AE}(1-T_0/T) + Q_{H_2O}(1-T_0/T_s)$, j_Q is the current density when $Q_{TE} = 0$, and T_s is the temperature of the external heat source used to heat up H_2O. It is clearly seen from Fig. 3 that the electrolyzer works at the temperatures between 343 K and 363 K, $Q_{AE} < 0$, $Q_{TE} > 0$ in the region of $j < j_Q$, and $Q_{TE} < 0$ in the region of $j > j_Q$.

According to Fig. 1 and the above analysis, the efficiency of the system can be expressed as [33]

$$\eta = \frac{N_{H_2,out} LHV}{P + Q_{H_2O}(1 - \frac{T_0}{T_s})}, \quad (9)$$

where *LHV* is the lower heating value of H_2.

It is worthwhile to point out that besides Fig. 1, one can design some new configurations for an alkaline water electrolyzer system, as shown in Fig. 4.

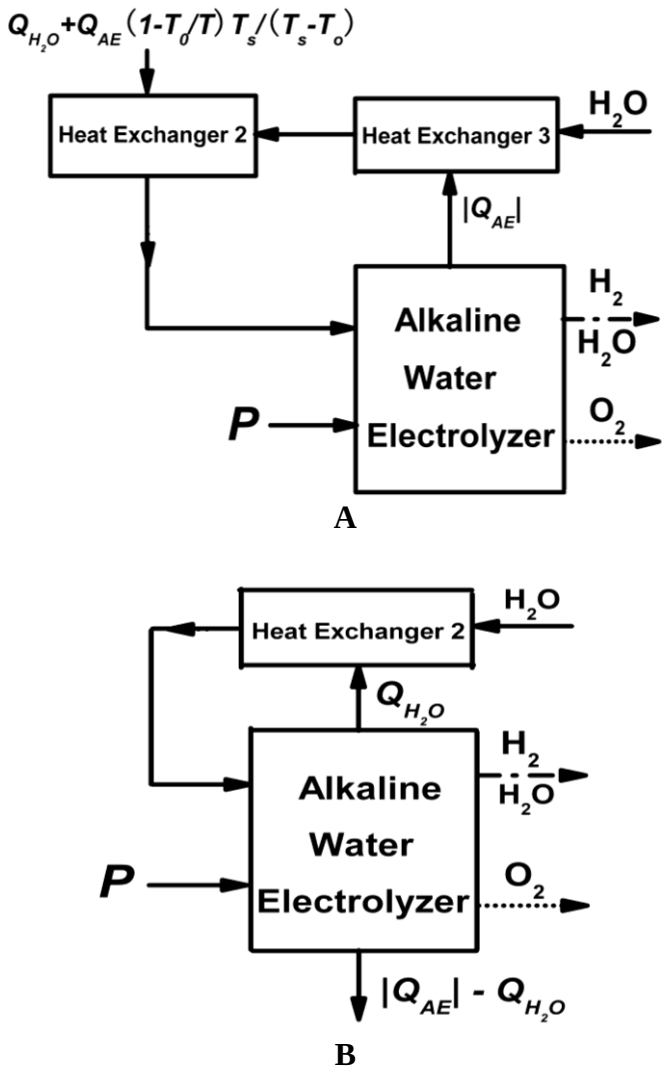

Figure 4. The part schematic diagrams of an alkaline water electrolyzer system for hydrogen production with (A) $Q_{TE} \geq 0$ and (B) $Q_{TE} < 0$. The other parts of the system are the same as those in Fig. 1.

It is seen from Fig. 4(A) that when $Q_{AE} < 0$ and $Q_{TE} \geq 0$, the surplus heat $|Q_{AE}|$ generated in the electrolyzer may be used to heat the water through an additional heat exchanger, i.e., heat exchanger 3 shown in Fig. 4(A). The heat $|Q_{AE}|(1-T_0/T)T_s/(T_s-T_0)$, which has the same temperature level as the

external heat source connected to heat exchanger 2, is transferred to the water, so that the heat supplied by the external heat source may be reduced from Q_{H_2O} to $Q_{H_2O}-|Q_{AE}|(1-T_0/T)T_s/(T_s-T_0)$. In such a case, the efficiency of the system can be expressed as

$$\eta=\frac{N_{H_2,out}LHV}{P+Q_{AE}(1-\frac{T_0}{T})+Q_{H_2O}(1-\frac{T_0}{T_s})}. \quad (10)$$

It is seen from Fig. 4(B) that when $Q_{AE}<0$ and $Q_{TE}<0$, one part of the surplus heat $|Q_{AE}|$ may be used to replace the heat Q_{H_2O} supplied by the external heat source and to heat the water so that the temperature of the water attains that of the electrolyzer, and the other part of the surplus heat $|Q_{AE}|$ is released to the environment.

The heat transferred from the electrolyzer to heat exchanger 2 is equal to $Q_{H_2O}=|Q_{AE}|(1-T_0/T)T_s/(T_s-T_0)$, which has the same temperature level as the external heat source, and the heat released to the environment is $[|Q_{AE}|-Q_{H_2O}]=|Q_{AE}|[1-(1-T_0/T)T_s/(T_s-T_0)]$. In such a case, neither Eq. (9) nor Eq. (10) may be directly used to calculate the efficiency of the system, while the efficiency of the system should be determined by

$$\eta=\frac{N_{H_2,out}LHV}{P}. \quad (11)$$

Equations (9)-(11) clearly show that the performance of an alkaline water electrolyzer depends on a set of thermodynamic and electrochemical parameters such as the operating temperature, current density, electrolyte thickness, electrolyte concentration, and so on. The related parameters are summarized in Table 2, and these parameters are kept constant in the following calculation unless mentioned specifically.

4. OPTIMIZATION ON THE PERFORMANCE OF AN ALKALINE WATER ELECTROLYZER

Using Eqs. (9)-(11), one can obtain the curves of the efficiency versus the current density, as shown in Fig. 5, where curves I and II correspond to the systems shown in Figs. 1 and 4, respectively. It is seen from Fig. 5 that the efficiency first increases and then decreases as the current density is increased. When the current density approached to the limiting current density, the efficiency decreases quickly. Moreover, the efficiency of the system (Curve II) shown in Fig.4 is larger than that (Curve I) shown in Fig. 1. It is natural because the redundant heat $|Q_{AE}|$ generated in the alkaline water electrolyzer is utilized in the systems shown in Fig. 4. Below, we will only discuss the performance of the systemic configurations shown in Fig. 4.

It is also seen from Fig. 5 that for an alkaline water electrolyzer system, there is a maximum efficiency $\eta_{\max}$ and a corresponding current density j_m. When $\eta < \eta_{\max}$, there always exist two corresponding current densities for a given efficiency, where one is smaller than j_m and the other is larger than j_m. Under the same efficiency, one always hopes to obtain a higher H_2 production rate $N_{H_2,out}$.

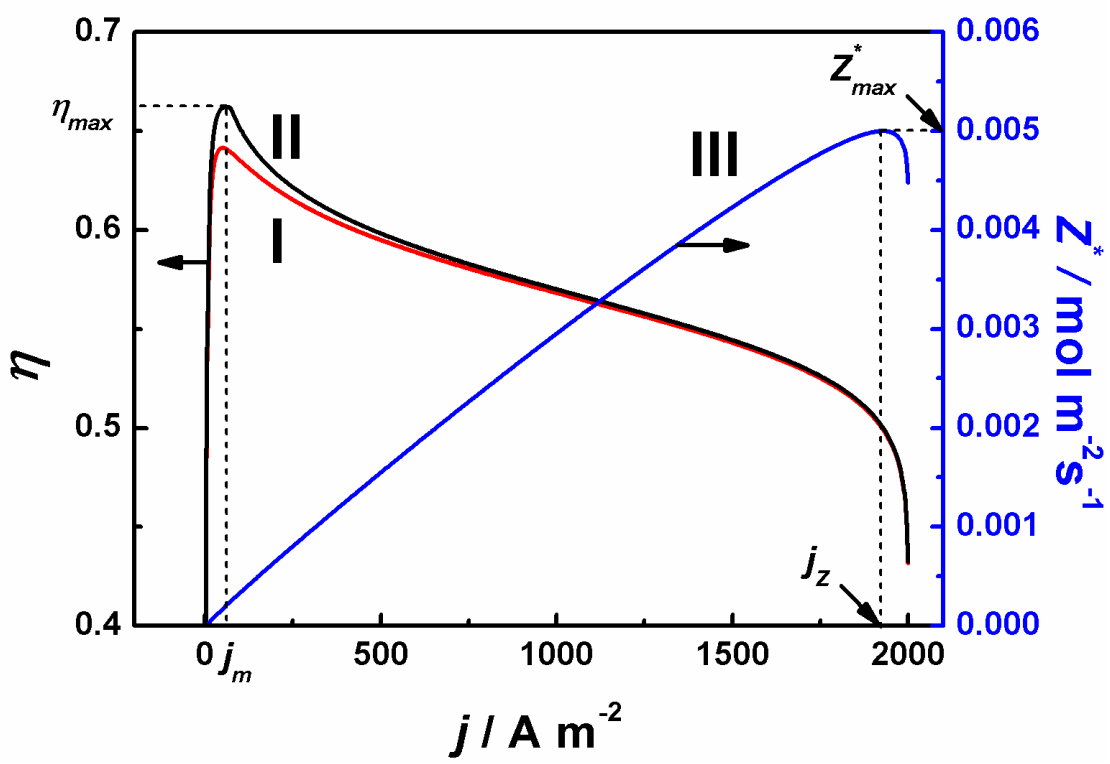

Figure 5. The curves of the efficiency and new multi-objective function varying with the current density for different configurations, where curve I corresponds to the system shown in Fig. 1, curves II and III correspond to the systems shown in Fig. 4, and j_m and j_Z are the current densities at the maximum efficiency $\eta_{\max}$ and maximum new multi-objective function $Z_{\max}$, respectively.

According to Faraday's law, the rate of electrochemical reaction υ is determined by $\upsilon = I/(n_e F)$ [18, 33, 42], and consequently, the production rate of H_2 can be expressed as

$$N_{H_2,out} = \frac{jA_e}{n_e F}. \qquad (12)$$

Equation (12) indicates clearly that the hydrogen production rate is proportional to the current density. Thus, taking into account both the efficiency and the hydrogen production rate, one can determine that the optimal current density should be located in the region of

$$j \geq j_m . \qquad (13)$$

When the system is operated in this region, the hydrogen production rate $N_{H_2,out}$ will increase as the efficiency η is decreased, and vice versa. Thus, in the optimal region of $j \geq j_m$, the reasonable choice of both the efficiency η and the hydrogen production rate $N_{H_2,out}$ must be still considered simultaneously. Equations (10)-(12) just provide some theoretical bases for solving this problem. Using Eqs. (10)-(12), we may introduce a multi-objective function as [43-45]

$$Z = \eta N_{H_2,out}, \qquad (14)$$

which is the product of the efficiency η and the hydrogen production rate $N_{H_2,out}$. Curve III in Fig. 5 shows the characteristics of the new multi-objective function varying with the current density, where $Z^* = Z / A_e$, $Z^*_{\max}$ is the maximum value of Z^*, and j_Z is the current density corresponding to $Z^*_{\max}$. It is seen from Fig. 5 that the new multi-objective function first increases and then decreases as the current density is increased. In the region of $j > j_Z$, the efficiency decrease quickly as the current density is increased. It results in a net decrease of the new multi-objective function. Thus, one can further determine that, in general, j_Z is the upper bound of the optimized current density and the system should be operated in the region of

$$j_m \leq j \leq j_Z . \qquad (15)$$

5. EFFECTS OF SOME PARAMETERS ON THE PERFORMANCE OF THE SYSTEM

Obviously, the performance of an alkaline water electrolyzer depends on a set of thermodynamic and electrochemical parameters. Below, we will discuss the effects of some important parameters on the performance of the system.

Figure 6(A) shows the influence of the operating temperature on the performance of the system. In the region of $j_m \leq j \leq j_Z$, the efficiency of the system increases as the operating temperature is increased. The maximum efficiency and the current density at the maximum efficiency also increase with the increase of the operating temperature. It may be explained as follows. At higher operating temperatures, the electrodes of the electrolyzer are more reactive, leading to a higher exchange current density and thus a lower activation overpotential. Moreover, as the operating temperature is increased, the mass transfer within the electrolyzer is improved so that there is a net decrease of the resistance. As a result, the input voltage decreases with the increase of temperature and it results in a reduced electrical energy input.

Figure 6(B) shows the influence of the electrolyte thickness on the performance of the system. In the region of $j_m \leq j \leq j_Z$, the efficiency of the system decreases as the electrolyte membrane thickness is increased. The larger the current density is, the larger the influence of the electrolyte membrane thickness on the efficiency of the system. This phenomenon can be explained as follows:

the thicker the electrolyte membrane is, the larger the ohm overpotential losses and the electrical energy input. It necessarily results in a lower efficiency for a thicker electrolyte membrane.

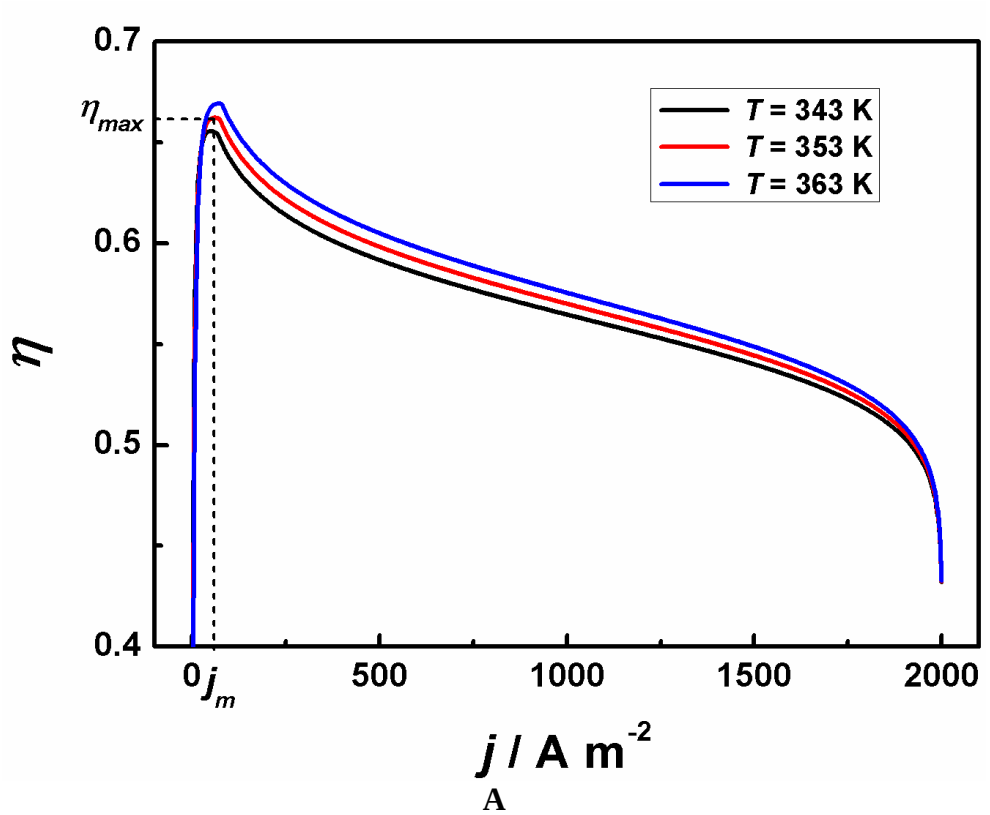

A

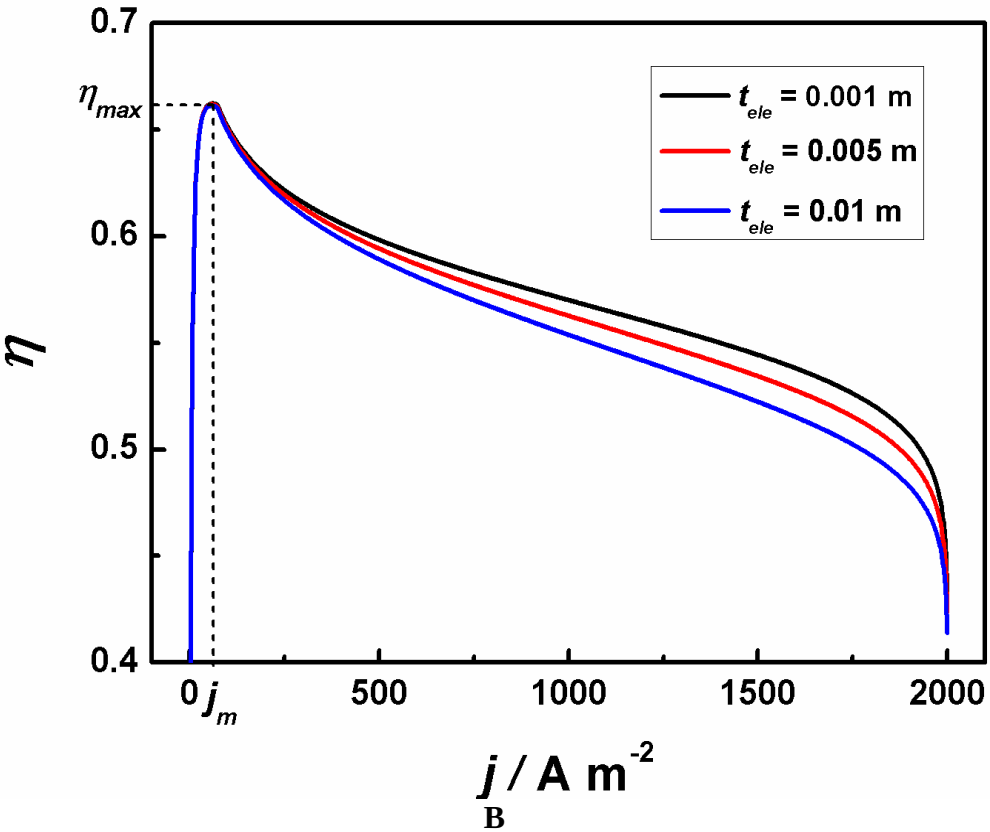

B

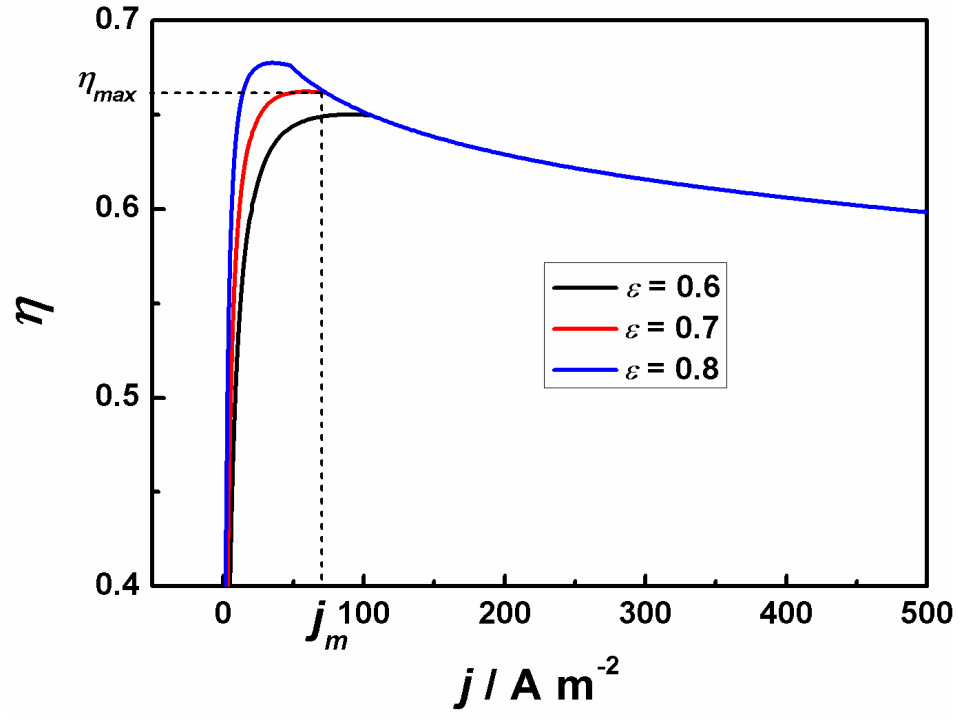

C

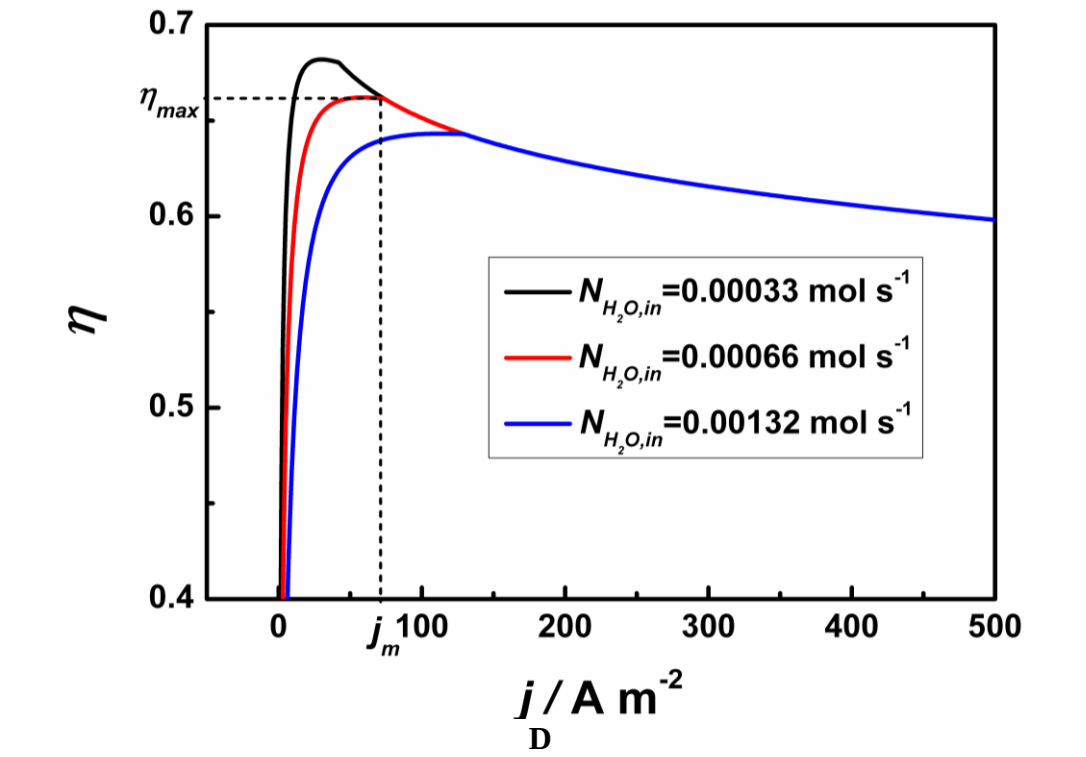

D

Figure 6. The efficiency versus current density curves for different (A) operating temperatures, (B) electrolyte membrane thickness, (C) effectiveness of the heat exchangers, and (D) inlet flow rates of H_2O, where j_m is the current density at the maximum efficiency η_{max}.

Figure 6(C) shows the influence of the effectiveness of the heat exchangers on the performance of the system. The efficiency of the system increases as the effectiveness of the heat exchangers is

increased. However, the influence mainly happens in the vicinity of $j = j_m$. When j is large, $|Q_{AE}|$ is much larger than Q_{H_2O} so that the influence of the effectiveness of the heat exchangers is negligible.

Figure 6(D) shows the influence of the inlet flow rate of H_2O on the performance of the system. The efficiency of the system decreases as the inlet flow rate of H_2O is increased. The influence mainly happens in the vicinity of $j = j_m$, while the influence of the inlet flow rate of H_2O is negligible in the other regions.

6. CONCLUSIONS

Based on semi-empirical equations and thermodynamic-electrochemical analyses of an alkaline water electrolyzer system, the performance of the system is evaluated and optimized. It is found that when the electrolyte concentration is increased, the input voltage of the electrolyzer first decreases and then increases for other given parameters. The result will be helpful to find one optimal value of the electrolyte concentration so that the input voltage of the electrolyzer obtains its minimum value. It is confirmed that the Joule heat resulting from the irreversibilities inside the electrolyzer is larger than the additional heat needed in the water splitting process. Moreover, some new configurations of an alkaline water electrolyzer system are put forward. It is found that the performance of the new configurations is better than that of the system that the redundant heat is directly released into the environment. According to the performance characteristics of the new configurations, the lower bound of the operating current density is determined. By considering both the efficiency and the hydrogen production rate of the system, a multi-objective function is introduced to further optimize the performance of the system, and consequently, the upper bound of the operating current density is also determined. Finally, the influence of some parameters on the performance of the alkaline water electrolyzer system operated in the optimal region is discussed in detail. The results obtained here may provide some guidance for the optimum design and operation of practical alkaline water electrolyzer systems for hydrogen production.

ACKNOWLEDGEMENTS
This work has been supported by the National Natural Science Foundation (No. 51076134) and the Fundamental Research Fund for the Central Universities, People's Republic of China.

References

1. Y. Kiros, *Int. J. Electrochem. Sci.*, 2(2007)285.
2. M. Perez-Page, V. Perenz-Herranz, *Int. J. Electrochem. Sci.*, 6(2011)492.
3. C. M. Bautista-Rodríguez, M. G. A. Rosas-Paleta, J. A. Rivera-Marquez, N. Tepale-Ochoa, *Int. J. Electrochem. Sci.*, 6(2011)256.
4. L. G. Carreiro, A. A. Burke, L. Dubois, *Fuel Process. Technol.*, 91 (2010) 1028.
5. C. Zamfirescu, I. Dincer, *Fuel Process. Technol.*, 86 (2005) 1279.
6. J. M. Gomes Antunes, R. Mikalsen, A. P. Roskilly, *Int. J. Hydrogen Energy*, 34 (2009) 6516.
7. M. Balat, *Int. J. Hydrogen Energy*, 33 (2008) 4013.

8. W. M. Martínez, A. M. Fernández, U. Cano, J. A. Sandoval, *Int. J. Hydrogen Energy*, 35 (2010) 8457.
9. J. C. Ganley, *Int. J. Hydrogen Energy*, 34 (2009) 3604.
10. J. Armor, *Appl. Catal. A: Gen.*, 176 (1999) 159.
11. M. Levent, D. Gunn, M. El-Bousiffi, *Int. J. Hydrogen Energy*, 28 (2003) 945.
12. J. Xu, C. Yeung, J. Ni, F. Meunier, N. Acerbi, M. Fowles, S C. Tsang, *Appl. Catal. A: Gen.*, 345 (2008) 119.
13. W. Balthasar, *Int. J. Hydrogen Energy*, 9 (1984) 649.
14. C. J. Winter, *Int. J. Hydrogen Energy*, 30 (2005) 681.
15. V. A. Goltsov, T. N. Veziroglu, *Int. J. Hydrogen Energy*, 26 (2001) 909.
16. L. Barreto, A. Makihira, K. Riahi, *Int. J. Hydrogen Energy*, 28 (2003) 267.
17. M. Liu, B. Yu, J. Xu, J. Chen, *J. Power Sources*, 177 (2008) 493.
18. M. Ni, M. K. H. Leung, D. Y. C. Leung, *Int. J. Hydrogen Energy*, 32 (2007) 4648.
19. M. Wang, Z. Wang, Z. Guo, *Int. J. Hydrogen Energy*, 35 (2010) 3198.
20. M. T. Balta, I. Dincer, A. Hepbasli, *Int. J. Hydrogen Energy*, 35 (2010) 4949.
21. B. Pierozynski, *Int. J. Electrochem. Sci.*, 6(2011)63.
22. M. Jayalakshmi, W. Y. Kim, K. D. Jung, O. S. Joo, *Int. J. Electrochem. Sci.*, 3 (2008) 908.
23. K. Zeng, D. Zhang, *Prog. Energy Comb. Sci.*, 36 (2010) 307.
24. O. Ulleberg, *Int. J. Hydrogen Energy*, 28 (2003) 21.
25. R. Solmaz, G. Kardas, *Electrochim. Acta*, 54 (2009) 3726.
26. M. Popczyk, J. Kubisztal, A. Budniok, *Electrochim. Acta*, 51 (2006) 6140.
27. R. Solmaz, A. Döner, G. Kardas, *Int. J. Hydrogen Energy*, 34 (2009) 2089.
28. F. Rosalbino, D. Macciò, E. Angelini, A. Saccone, S. Delfino, *J. Alloys Compd*., 403 (2005) 275.
29. L. Zhou, Y. F. Cheng, *Int. J. Hydrogen Energy*, 33 (2008) 5897.
30. C. Bailleux, *Int. J. Hydrogen Energy*, 6 (1981) 461.
31. A.Ferreira, E. Conzalez, E. Ticianelli, L. Avaca, B. Matvienko, *J. Appl. Electrochem*., 18 (1988) 894.
32. H. Zhang, G. Lin, J. Chen, *Energy*, 2011, doi: 10.1016/j.energy.2011.04.009.
33. H. Zhang, G. Lin, J. Chen, *Int. J. Hydrogen Energy*, 35(2010)10851.
34. R. H. Perry, C. H. Chilton, *Chemical Engineering's Handbook*, 5th ed. McGraw Hill Kogakusha, Ltd., Tokyo (1973).
35. R. O'Hayre, S. W. Cha, W. Colella, F. B. Prinz, *Fuel Cell Fundamentals*, John Wiley & Sons Ltd., New York (2006).
36. A.Ursúa, L. Marroyo, E. Gubía, L. M. Gandía, P. M. Diéguez, P. Sanchis, *Int. J. Hydrogen Energy*, 34 (2009) 3221.
37. P. M. Diéguez, A. Ursúa, P. Sanchis, C. Sopena, E. Guelbenzu, L. M. Gandía, *Int. J. Hydrogen Energy*, 33 (2008) 7338.
38. I.Verhaert, M. De Paepe, G. Mulder, *J. Power Sources*, 193 (2009) 233.
39. Y. Zhao, C. Ou, J. Chen, *Int. J. Hydrogen Energy*, 33 (2008) 4161.
40. R. J. Gilliam, J. W. Graydon, D. W. Kirk, S. J. Thorpe, *Int. J. Hydrogen Energy*, 32 (2007) 359.
41. M. Ni, M. K. H. Leung, D. Y. C. Leung, *Energy Convers. Manage*., 49 (2008) 2748.
42. S. J. Watowich, R. S. Berry, *J. Phys. Chem.*, 90 (1986) 4624.
43. H. Zhang, G. Lin, J. Chen, *Int. J. Hydrogen Energy*, 36 (2011)4015.
44. W. Na, B. Gou, *J. Power Sources*, 166 (2007) 411.
45. S. M. C. Ang, D. J. L. Brett, E. S. Fraga, *J. Power Sources*, 195 (2010) 2754.